Temperature Measurement from the Translational Kinetic Energy Release Distribution in Cluster Dissociation: A Theoretical Investigation†

F. Calvo*

Laboratoire de Physique Quantique, IRSAMC, Université Paul Sabatier, 118 Route de Narbonne, F31062 Toulouse Cedex, France

P. Parneix

Laboratoire de Photophysique Moléculaire, CNRS, Fédération de Recherche Lumière Matière, Bât. 210, Université Paris-Sud, F91405 Orsay Cedex, France

F. X. Gadéa

Groupe NanoScience, CEMES, UPR 8011, 29 rue J. Marvig, BP 94347, 31055 Toulouse Cedex 4, France

Received: July 12, 2005; In Final Form: September 23, 2005

Unimolecular dissociation of neutral and charged argon clusters is theoretically investigated in the context of calorimetric measurements. The temperature of the product cluster is estimated from the distribution of the translational kinetic energy released (KER), assumed to have the form $f(\epsilon) \approx \epsilon^{\alpha} \exp(-\epsilon/k_B T)$. Phase space theory (PST) in its orbiting transition state (OTS) version is validated by comparing its predictions to the results of large-scale molecular dynamics simulations. The temperatures estimated from the KER distributions are seen to be generally lower than the actual microcanonical temperature computed from independent Monte Carlo simulations of the product cluster at thermal equilibrium. On the basis of these deviations, the various approximations leading from the rigorous PST/OTS treament to the assumed exponential form are critically discussed. In the case of Ar_n^+ clusters, the use of a quantum diatomic-in-molecules Hamiltonian constructed from recent ab initio calculations reveals some possible inadequacies of the $1/r^4$ ion/dipole interaction at intermediate distances due to some residual charge transfer.

I. Introduction

The properties of free atomic clusters have long been obtained from spectroscopy performed in molecular beams. While a size selection is necessary to get insight at the atomic resolution, the difficulty in estimating the temperature has often hindered precise measurements. Temperature is an important parameter that has been shown to influence optical[1] and chemical[2] properties, and also structure itself[3] through variations in the mass abundance spectra. Since the seminal work by Gspann,[4] special attention to cluster temperature has been paid by several groups, through dedicated calorimetric experiments[5−10] aiming at probing phase transitions.

Direct vibrational or rotational spectroscopies are essentially restricted to small systems.[11] One other route for measuring cluster temperatures comes from the analysis of the fragmentation patterns. The Haberland group[5] and more recently the Jarrold group[9] have used the distribution of products in photo- or collision-induced fragmentations as a way of determining temperatures. At lower excitations, the distribution of kinetic energy released after dissociation carries a lot of information about the energetics and kinetics of the reactions.[12] In general, the binding energies or temperatures are deduced in experiments[13−19] through a comparison with some established statistical rate theories[20] such as those pioneered by Weisskopf[21] or by Rice, Ramsperger, and Kassel (RRK).[22] Significant progress was made by Klots[23−26] who developed the quasi-equilibrium theory (QET) of unimolecular decomposition and later introduced the concept of the "evaporative ensemble". Klots also emphasized the role of angular momentum constraints in the calculation of the kinetic energy released and the rate constant. This work, as well as contributions by Troe[27] and especially Chesnavich and Bowers,[28] among others, contributed to the development of the so-called phase space theory (PST) initiated by Nikitin[29] and Light and co-workers.[30] Both the QET and PST approaches have since achieved large success by providing a theoretical framework for experimental interpretations (for early reports, see, e.g., refs 31 and 32). Beyond unimolecular decomposition, thermionic emission[33] can also be interpreted using statistical theories.[34] Recent experiments in the Bordas group have reported temperature measurements in the electronic emission from small tungsten[35] and carbon[36] clusters.

However, the predictive capacities of these powerful theories are limited by the presence of several factors that are undetermined, or hard to guess. For instance, it was noted by Matt and co-workers[37] that the binding energy of C_{60}^+ associated to the loss of C_2 could differ by more than 10 eV because of the poor knowledge of the transition state energy.

An alternative way to assess statistical rate theories is to perform trajectory calculations using molecular dynamics simulations. In cluster science, this approach has been put forward by Weerasinghe and Amar[38] who compared the predictions of the RRK and PST theories for the unimolecular evaporation of rare-gas systems. Peslherbe and Hase extended

† Part of the special issue "William Hase Festschrift".

* Corresponding author.

10.1021/jp0538114 CCC: $33.50
Published on Web 10/28/2005

these conclusions to the case of aluminum clusters.[39−42] In particular, they considered zero-point corrections as well as nonzero total angular momenta. The general conclusion of these works is that phase space theory is quantitative in reproducing statistical and kinetic properties of dissociating clusters, provided that angular momentum constraints and anharmonicities of the vibrational density of states are correctly accounted for.[38−42] In comparison, the simpler RRK[22] or Engelking[13] theories significantly underestimate or overestimate both the kinetic energy released and the rate constant, the latter by several orders of magnitude.

More recently, we investigated the performances of PST in a broader range of situations.[43−46] Rotating systems and the rotational cooling and heating effects[47] were studied on model rare-gas clusters.[43] Molecular,[44] heterogeneous,[45] and asymmetrical[46] clusters were also considered. In all these situations, PST was again seen to give a very good agreement with respect to molecular dynamics trajectories, that can be considered numerically exact, provided that enough events have been gathered. It thus seems that the maturity reached by PST allows its predictions to be used quite safely as a benchmark with respect to more approximative treatments. In the present work, we focus on the distribution of translational kinetic energy released upon dissociation of Ar_n and Ar_n^+ clusters. Our motivation is to establish connections between these distributions and the thermodynamical state of the product cluster. By relying on Monte Carlo and molecular dynamics sampling, the thermodynamical properties can be fully calculated and compared to the estimates from the dissociation patterns.

The choice of neutral argon clusters comes from the requirement for simple atomistic models and heavy sampling. The Lennard-Jones (LJ) potential allows us to investigate relatively large clusters such as Ar_{56} for various total energies. The cationic cluster Ar_{14}^+ is more realistic but also more demanding from the computational point of view. A diatomic-in-molecules (DIM) quantum Hamiltonian built from state-of-the-art spectroscopic data[48] provides an appropriate model for statistical and dynamical purposes.

The paper is organized as follows. The main elements of statistical theory are summarized in the next section. We pay particular attention to the approximations introduced in the derivation of the Arrhenius expression for the KER distribution, $f(\epsilon) \propto \epsilon^{\alpha} \exp(-\epsilon/k_B T)$. Our results are presented and discussed in section III, and possible improvements for using this basic form in interpreting experiments are proposed. We finally summarize and conclude in section IV.

II. Theory

We consider the general unimolecular dissociation of an atomic cluster, $X_{n+1} \rightarrow X_n + X$. The total energy E of the parent cluster X_{n+1} is partitioned upon dissociation into the following terms:

$$E = E_0 + \epsilon_t + \epsilon_r + \epsilon_v = E_0 + \epsilon_{tr} + \epsilon_v \qquad (1)$$

where E_0 is the dissociation energy (or difference in binding energy between the parent and product clusters), ϵ_t and ϵ_r are the translational and rotational relative kinetic energies of the product, and ϵ_v is its remaining internal (vibrational) energy. In the case of dissociation into compounds, both larger than a single atom, the rotational and vibrational energies would be shared by the two products. Similarly, the total angular momentum J is partitioned into the orbital momentum L and the individual momenta after dissociation J_1 and J_2 as the vectorial sum $J = J_1 + J_2 + L = J_r + L$.

In the present work, we assume that the clusters have no initial angular momentum. Within the PST formalism, the unnormalized probability $f(\epsilon_t)$ that a dissociation event occurs with translational kinetic energy released ϵ_t is given by integration over all possible values of the rotational energy ϵ_r as[28]

$$f(\epsilon_t) \propto \int_0^{A(\epsilon_t)} \frac{\partial \Gamma}{\partial \epsilon_r}\, \omega(E - E_0 - \epsilon_t - \epsilon_r)\, d\epsilon_r \qquad (2)$$

Here, we have denoted $\omega(E)$ the vibrational density of states (VDOS) of the product cluster at energy E and $\Gamma(\epsilon_r, \epsilon_t)$ the rotational density of states (RDOS) of the two products. $A(\epsilon_t)$ is the maximum value of the rotational energy available because of angular momentum constraints. In PST/OTS, the transition state is located at the products, and a centrifugal barrier $\epsilon^{\dagger}(L)$ has to be overcome. Because the orbital momentum exactly compensates the internal momentum, this defines a maximum value for J_r denoted as J_r^{max} such that $\epsilon^{\dagger}(J_r^{max}) = \epsilon_t$. In turn, J_r^{max} is related to $A(\epsilon_t)$. The product clusters investigated in the present work will be essentially considered as spherical tops. By denoting B their rotational constant, the RDOS is expressed as[20] $\Gamma = \epsilon_r/B = J_r^2$, and $A(\epsilon_t)$ is given by $B(J_r^{max})^2$.

At this stage, the kinetic energy distributions do not carry any explicit information about the temperature of the product. Clearly, the thermodynamical information is contained into the vibrational DOS ω; hence, some approximations are needed. Below, these approximations will be referred to as (A1)−(A4) for clarity.

(A1) In general, $\epsilon_{tr} = \epsilon_t + \epsilon_r$ is much smaller than the available energy $E - E_0$.[52] This will be especially true for large systems, for which E scales linearly with the number of atoms n, but ϵ_{tr} remains limited. We can thus perform a Taylor expansion of ω up to second order in ϵ_{tr}, and we find

$$\omega(E - E_0 - \epsilon_t - \epsilon_r) = \omega(E - E_0)\left[1 - \frac{\epsilon_{tr}}{k_B T_\mu} + \left(1 - \frac{k_B}{C}\right)\frac{\epsilon_{tr}^2}{2k_B^2 T_\mu^2} + \mathcal{O}(\epsilon_{tr}^3)\right] \qquad (3)$$

with k_B being the Boltzmann constant. In writing eq 3, we have introduced the microcanonical temperature T_μ defined as

$$\frac{1}{k_B T_\mu} = \frac{\partial \ln \omega}{\partial E} \qquad (4)$$

and the microcanonical heat capacity $C = \partial E/\partial T_\mu$.

(A2) We further assume that the heat capacity C is much larger than k_B. Again, this approximation will be mostly valid for larger clusters.[53] In doing so, the Taylor expansion of the VDOS is assimilated to that of an exponential form, hence

$$\omega(E - E_0 - \epsilon_t - \epsilon_r) \approx \omega(E - E_0) \exp(-\epsilon_{tr}/k_B T_\mu) \qquad (5)$$

Inserting this expression into the integral of eq 2, one finds

$$f(\epsilon_t) \propto [1 - \exp(-A(\epsilon_t)/k_B T_\mu)] \exp(-\epsilon_t/k_B T_\mu) \qquad (6)$$

The latter form cannot be fully exploited to extract T_μ from f, because $A(\epsilon_t)$ is not known yet.

(A3) The dissociation potential felt by the fragments X_n and X can be generally approximated as $V(r) = -C_p/r^p$, with $p = 4$ (ion/neutral) or $p = 6$ (neutral/neutral). The centrifugal barrier is then given by the well-known Langevin theory[54]

$$A(\epsilon_t) = \Lambda_p \epsilon_t^{(p-2)/p} \quad (7)$$

with Λ_p a constant given by $\Lambda_p = p\mu B C_p^{2/p}[2/(p-2)]^{(p-2)/p}$ and μ being the reduced mass.

It is instructive to look at the size dependence of Λ_p. For a neutral/neutral dissociation, $C_6 \propto n$ and $B \propto n^{-5/3}$, therefore Λ_6 is proportional to $n^{-4/3}$. For an ion/neutral reaction, C_4 remains constant with n and $\Lambda_4 \propto n^{-5/3}$. In both cases, $A(\epsilon_t)$ decreases with n at least as rapidly as $1/n$.

(A4) Under the large size assumption of $n \gg 1$, and considering the aforementioned conditions, the first term in the right-hand side of eq 6 can be approximated as $1 - \exp[-\beta A(\epsilon_t)] \approx \beta A(\epsilon_t)$, leading to the simple form for the KER

$$f(\epsilon_t) \propto \epsilon_t^{(p-2)/p} \exp(-\epsilon_t/k_B T_\mu) \quad (8)$$

This is the conventional expression used to extract a temperature from experimental kinetic energy distributions. From our derivation, similar to that of Klots,[26] it is clear that the choice of an $\epsilon^\alpha \exp(-\epsilon/k_B T)$ form relies on a series of approximations that can be summarized as follows.

(i) The large size approximations (A1) and (A2): the vibrational density of states is Taylor expanded up to second order, leading to the Arrhenius form including the microcanonical temperature; the heat capacity is assumed to be very large with respect to k_B.

(ii) The dissociation potential is radial with the form $-C_p/r^p$: this leads to the expression $A(\epsilon) \propto \epsilon^{(p-2)/p}$ for the centrifugal barrier energy (approximation (A3)).

(iii) The angular momentum constraints (A4): the maximum rotational energy $A(\epsilon)$ available after crossing the centrifugal barrier is explicitly included, but assumed to be small $(1 - e^{-\beta A} \simeq \beta A)$.

In the literature, KER distributions have often been adjusted to an $\epsilon \times \exp(-\epsilon/k_B T)$ form, even for clusters.[8] As noted previously,[26] this expression would only be valid for hard core systems ($p \rightarrow \infty$, cf., eq 8) or for macroscopic objects for which the constraints on angular momentum are released. While both α and T can be fitted independently from the distribution, an estimate of the temperature is obtained from the first moments $M_1 = \langle \epsilon_t \rangle$ and M_2 only, without any assumption on the power α

$$k_B T_\mu = \frac{\langle \epsilon_t^2 \rangle - \langle \epsilon_t \rangle^2}{\langle \epsilon_t \rangle} = M_2 \quad (9)$$

with $\langle\ \rangle$ denoting an average over the distribution f. The second moment is related to the heat capacity of the system through the energy fluctuations in the numerator of eq 9. However, while the heat capacity was assumed to be large, M_2 remains limited, because the denominator $\langle \epsilon_t \rangle$ scales similarly (that is linearly) with the cluster size.

III. Results and Discussion

A. Neutral Argon Clusters. We start by looking at neutral Ar_n clusters. Such clusters will be used as model systems, for which the simplicity of the potential energy surface (PES) allows statistical theories to be accurately tested against molecular dynamics simulations. Two sizes have been considered, namely, $n = 14$ and $n = 56$, because of the highly spherical character of the main products.

1. Technical Details. The potential energy of neutral argon clusters has been taken as a sum of pairwise Lennard-Jones interactions with $\sigma = 3.405$ Å and $\epsilon = 120$ K. To test the accuracy of the PST formalism, MD simulations of evaporative trajectories have been carried out. For each excess energy, 5000 trajectories were propagated using a fifth-order Adams−Moulton predictor−corrector algorithm with a time step of 2 fs. Initial conditions were chosen at zero total angular momentum.

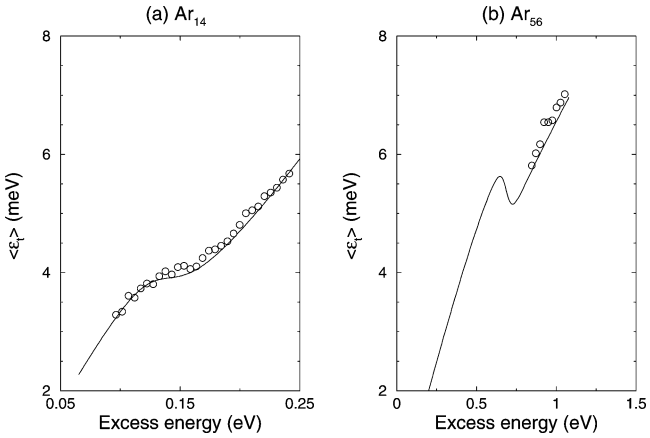

Figure 1. Average translational kinetic energy released upon dissociation of Ar_{n+1} clusters, as a function of energy above the dissociation threshold. (a) Ar_{14}; (b) Ar_{56}. The MD results are shown as symbols, and the PST/OTS predictions are given by the solid lines.

As seen in the previous section, one of the ingredients of a PST calculation is the vibrational density of states of the products. We have computed the vibrational densities of Ar_{13} and Ar_{55} from parallel tempering Monte Carlo simulations, using 50 replicas in the temperature range $1\ K \leq T \leq 50$ K, with 10^6 MC cycles per replica following $2 \cdot 10^5$ MC cycles for equilibration. Exchange moves were attempted after each cycle with 10% probability. The configurational densities were constructed from the potential energy distributions through a multiple histogram reweighting analysis.[49] The vibrational densities were subsequently obtained by convolution with the analytical kinetic DOS.[50]

A second important point in PST/OTS concerns the rotational densities of states. The potential felt by the dissociating atom is required for the calculation of the location and height of the centrifugal barrier. We have calculated this potential from a Monte Carlo simulation constrained at a series of fixed distance r between the atom and the center of mass of the product. The effective potential was fitted to a $-C_6/(r - r_0)^6$ form, with optimal parameters $C_6 = 0.6447$ eV Å^6 for Ar_{13} and $C_6 = 0.3061$ eV Å^6 for Ar_{55}, with radii $r_0 = 1.7$ Å for Ar_{13} and $r_0 = 5.89$ Å for Ar_{55}. Angular momenta and rotational energies are then related to each other from the rotational constant of the product, also obtained from the MC calculations. At $T = 36$ K, we find $B = 3.32 \cdot 10^{-3}$ cm^{-1} for Ar_{13} and $B = 3.1 \cdot 10^{-4}$ cm^{-1} for Ar_{55}. Because the potential does not have the simple $1/r^p$ form, one cannot calculate the centrifugal barrier exactly, and a numerical resolution is carried out.

2. Validation of PST. The predictions of PST/OTS are first tested against extensive MD simulations. A comparison between MD and PST/OTS for the average KER $\langle \epsilon_t \rangle$ is shown in Figure 1 for the two sizes. Standard deviations estimated from 10 independent sets of 5000 simulations are roughly the size of the symbols.

The very good agreement observed on this figure confirms the previous studies, which emphasized the ability of phase space theory to reproduce other observables such as the total kinetic energy release ϵ_{tr} or the rotational angular momentum J_r of the product cluster.[38−46] In the two systems, the variations of $\langle \epsilon_t \rangle$ versus excitation energy show a small change in

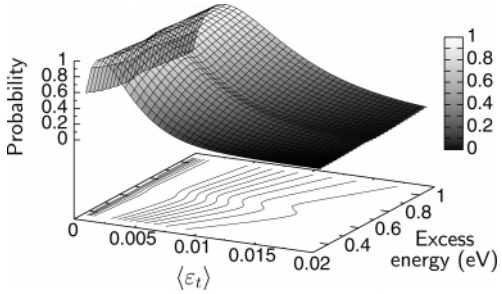

Figure 2. Kinetic energy release distribution upon dissociation of Ar_{56} obtained from PST/OTS, as a function of the excess energy. For each excess energy, the distribution is normalized at its maximum. The isolevel contour lines are also shown.

curvature, which signals the occurrence of the solidlike−liquidlike phase change, associated with dynamical coexistence in the microcanonical ensemble.[51] This feature is especially prominent in the dissociation of the larger cluster Ar_{56}, for which a backbending and a decrease of $\langle \epsilon_t \rangle$ take place close to 0.68 eV excess energy. Unfortunately, the large size of the system hampers the direct MD simulation of evaporation in this energy range, and we have not been able to check the PST results against MD. But this signature of a phase change is clearly seen in the numerical simulation data for Ar_{14}, confirming that fragmentation statistics carry important information about phase transitions.

In Figure 2, the KER distributions for the dissociation of Ar_{56}, obtained from the PST calculation, are shown in a broad range of excess energy as a two-dimensional plot. For convenience, the KERD are normalized at their maximum. This graph provides another view at the manifestations of the phase change on the kinetic energy distributions. Both the position of the maximum and the width exhibit non-monotonic changes across the solid−liquid transition. The isolevel contour lines at the base of the plot reproduce quite well the backbending of the microcanonical temperature and the average KER. These results clearly indicate that the changes in the distribution of energy released could be interpreted directly in terms of the phase change in the product cluster.

3. Calorimetric Measurements. From the different approximations described in the theoretical section, the microcanonical temperature of the product cluster may characterize the KER distribution obtained at a given excess energy, through the mathematical form $\epsilon_t^{\alpha} \times \exp(-\epsilon_t/k_B T)$. At this stage, one can adjust the available distribution as an Arrhenius law either by fitting α and T simultaneously, by fitting T only and assuming a specific value for α, or from the first two moments of the distribution (see eq 9). In the present case, the distributions have been adjusted to reproduce the PST distributions with $\alpha = {}^2/_3$ or $\alpha = 1$. While the former value is the natural choice for neutral/neutral products interacting through $1/r^6$ dispersion forces, the latter value was also considered, since it has been often used to interpret experimental data.[8] A justification for this value can be found in the Weisskopf formalism and neglecting the variations of the collision cross-section with respect to ϵ_t.

In Figure 3, typical MD and PST results for the KERD are shown along with the best fits obtained for the two values of the power α and for the two parent clusters Ar_{14} and Ar_{56}. Beyond the good agreement between MD and PST, the two fits with different α values show contrasting qualities. Contrary to the best distribution fitted with $\alpha = 1$, the distribution for $\alpha = {}^2/_3$ matches well the PST data.

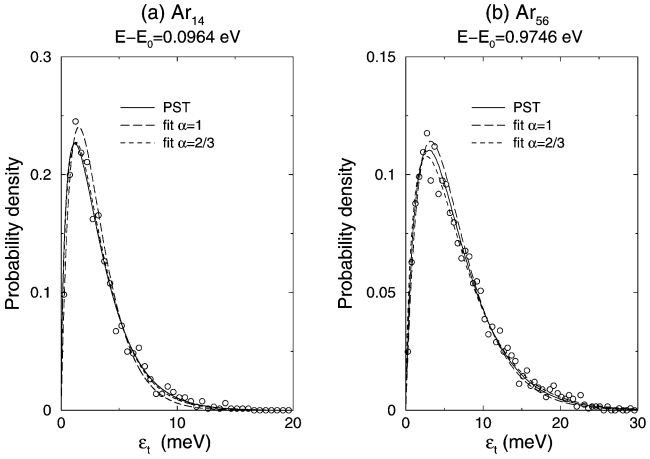

Figure 3. Examples of KER distributions for the dissociation of neutral Ar_{n+1} clusters with $n = 13$ (left panel) and $n = 55$ (right panel). The symbols refer to the MD results, the solid lines refer to the PST/OTS calculation, and the dashed lines represent the best fits to Arrhenius forms with powers 1 and $^2/_3$.

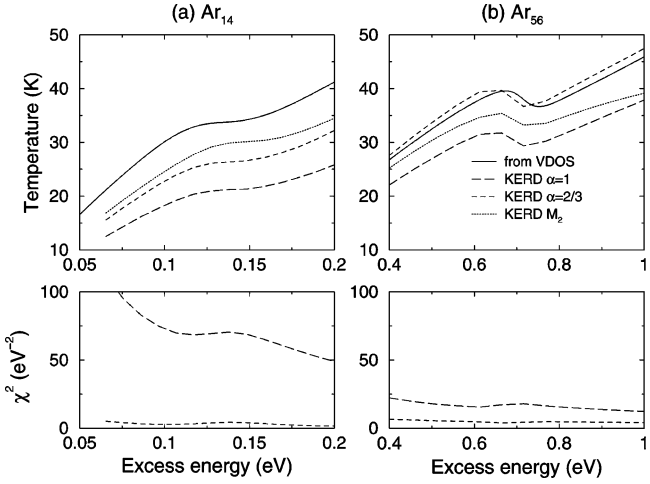

Figure 4. Temperature of the product cluster Ar_n vs excitation energy for $n = 13$ (left panel) and $n = 55$ (right panel). The reference value obtained from Monte Carlo simulations is given as solid lines, and several temperatures extracted from adjustment of the KER distributions are represented. The lower panels show the statistical error χ^2 corresponding to the best fit of the KER distribution to the Arrhenius form.

The adjustment of the KER distribution to Arrhenius forms was repeated for a series of excess energies and for the two neutral clusters. We have represented in Figure 4 the microcanonical temperature obtained from these best fits with the two powers α, as well as the temperatures given by the first moments of the distribution. These temperatures are compared with the thermodynamical value computed from the vibrational densities of states, by solving eq 4. The quality of the adjustment, as measured by the standard mean-square error χ^2, is also given in the lower panels of Figure 4. In accordance with our previous observation, the Arrhenius forms are much more appropriate for $\alpha = {}^2/_3$ than for $\alpha = 1$. In all cases, fitting the KERD to the Arrhenius expression with $\alpha = 1$ or estimating the temperature from the moments of the distribution leads to a significant underestimation of the temperature. The error in the determination of temperature is especially large for the smaller system, from about 15% with the moments calculation and reaching about 40% when fitting with $\alpha = 1$. For Ar_{56}, the agreement between the Arrhenius form with $\alpha = {}^2/_3$ and the

thermodynamical value is remarkably good, wiht the relative error always below 4% in the energy range considered here.

From the previous results, size effects are seen to be primarily responsible for the discrepancies between the PST distributions and their adjustment to an Arrhenius law, even when the correct power α is used (for the present neutral clusters, $\alpha = {}^2/_3$). The extraction of the temperature from the moments of the distribution is also not free of errors: while this method provides the best comparison for the small cluster, it is not as reliable as the plain Arrhenius fits for the larger system.

B. Charged Argon Clusters. We now turn to cationic clusters, which are experimentally more interesting, as they allow precise measurements through size selection. The group of Stace, in particular, have interpreted its experimental data on argon clusters using phase space theory.[55,56]

1. Technical Details. The charge on argon clusters is partially delocalized over a few atoms, and cationic clusters can be roughly seen as a charged ionic core solvated by atoms bound by dispersion and polarization forces.[57] Clearly, explicit pair potentials cannot give a good account for this partly covalent bonding. Fortunately, simple but highly accurate quantum Hamiltonians are available to describe the ground state (and the low-lying excited states) of charged rare-gas clusters. The diatomic-in-molecules (DIM) approximation[58] provides structural and dynamical properties in very good agreement with experiments. A complete presentation of the DIM Hamiltonian lies beyond the scope of the present paper, and we refer the reader to ref 57 for further information. The key ingredients of the DIM model are the potential energy curves for the ground states of Ar_2 and Ar_2^+, as well as the excited states curves for the charged dimer. We made some changes to the original Hamiltonian of ref 57 by including the more recent data by Wüest and Merkt[48] who fitted high-resolution photoelectron spectroscopy measurements to obtain curves corresponding to the first six electronic states of Ar_2^+.

Molecular dynamics simulations of the evaporation process $Ar_{n+1}^+ \rightarrow Ar_n^+ + Ar$ have been performed for $n = 13$ on the ground-state electronic surface, using a fourth-order Runge−Kutta propagator with time step of 0.4 fs. Again, the size $n = 13$ was chosen because of the roughly spherical shape of the main product. Because of the relatively heavy computational cost of the DIM model, we had to choose a high excitation energy corresponding to 100 K. Twenty thousand trajectories were generated from a low-energy (10 K) run, with each trajectory being stopped after an evaporation event taking place within 20 ps.

The PST/OTS analysis was carried out using the average rotational constant of the Ar_{13}^+ product at 30 K, namely, $B = 3.02 \cdot 10^{-3}$ cm^{-1}. The vibrational density of states was computed from parallel tempering Monte Carlo simulations in the canonical ensemble, using 50 replicas in the temperature range 1 K $\leq T \leq$ 150 K. The MC simulations consisted of $5 \cdot 10^5$ cycles following $2 \cdot 10^5$ cycles for each replica, with one exchange move attempted with 10% probability per cycle. For the radial potential, we also performed Monte Carlo simulations at fixed distance between the dissociating atom and the center of mass of the product. The results obtained at 10 K are represented in Figure 5 and compared to the exact long-range behavior $-C_4/r^4$ with $C_4 = 11.816$ eV Å^4 (ref 48), as well as to the better fit $-C_4/(r - r_0)^4$ with $r_0 = 2.34$ Å.

The deviations of the simulation data to the $1/r^4$ law are significant, especially at moderate distances. As in neutral systems, these deviations originate from the finite extent of the cluster, but also here from the partially covalent bonding at small distances. This is illustrated in the inset of Figure 5, where the average partial charge carried by the dissociating atom is plotted against its distance. The residual charge transfer at low distances exceeds 0.1, which is significant in this system where the interactions are otherwise of the dispersion type. Such a behavior is probably less likely to occur in larger charged clusters, because the charge delocalization remains limited in space to a core of 3−4 atoms.[57] The significant charge transfer makes the $-C_4/(r - r_0)^4$ expression poorly relevant at moderate distances, which might become a problem when the centrifugal barrier is located at short distances, as it would be for initially rotating clusters. The present simulations have been performed at zero initial angular momentum; we have thus kept the simple $-C_4/(r - r_0)^4$ form for the dissociation potential.

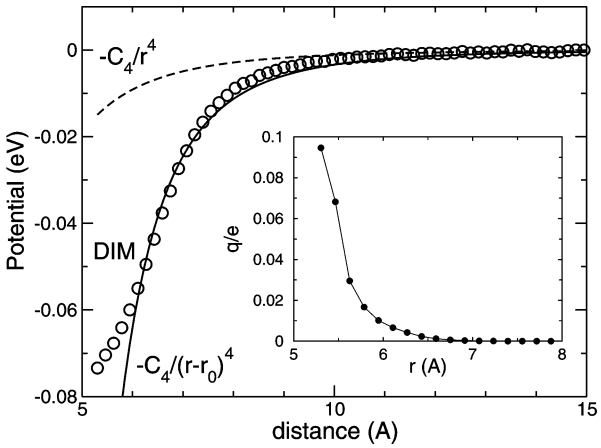

Figure 5. Radial potential felt by a neutral atom dissociating from Ar_{13}^+, as a function of its distance r to the cluster center of mass. The symbols are the results of Monte Carlo calculations at 10 K using the DIM Hamiltonian and constrained at fixed r. The dashed line is the $-C_4/r^4$ long-range potential; the solid line refers to the modified $-C_4/(r - r_0)^4$ potential actually used in the PST/OTS calculation. The inset shows the average charge carried by the dissociating atom vs r.

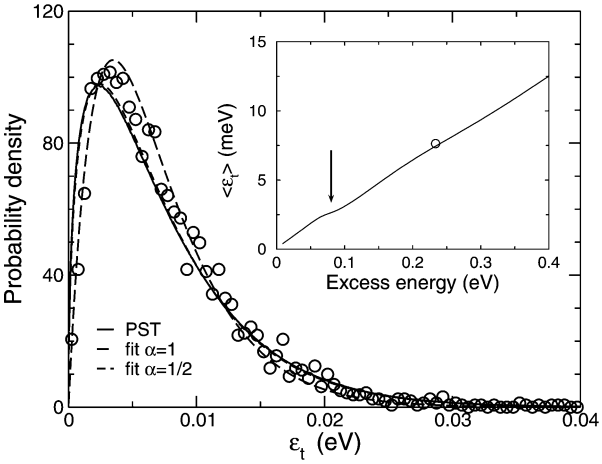

Figure 6. KER distribution for the dissociation of Ar_{13}^+ at excess energy $E - E_0 = 0.2367$ eV, obtained from MD simulations (symbols) or from the PST/OTS predictions (solid line). The best fits of the distribution to Arrhenius forms with powers 1 and $^1/_2$ are also shown as dashed lines. Inset: average translational kinetic energy released vs excess energy above dissociation threshold, from PST/OTS (solid line) and MD simulations (symbol). The arrow shows the location of the solidlike−liquidlike transition.

2. Validation of PST. The distributions of kinetic energy released upon evaporation of a neutral atom from Ar_{14}^+ at an excitation energy of 100 K are represented in Figure 6. We compare in this figure the results of microcanonical MD simulations to the PST/OTS calculation. The overall agreement

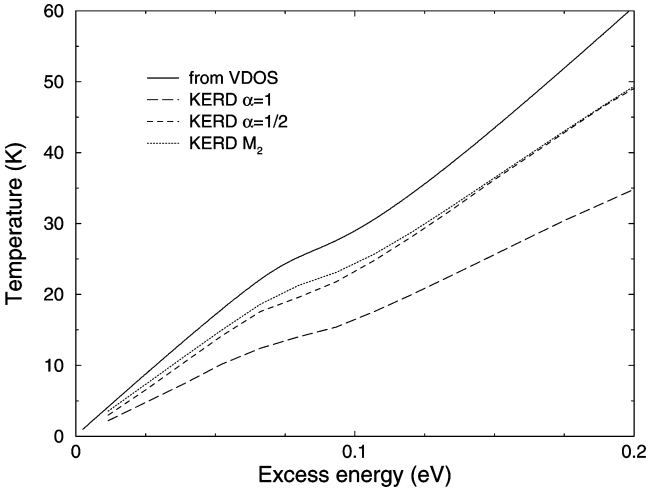

Figure 7. Temperature of the product cluster Ar_{13}^+ versus excitation energy, from Monte Carlo simulations (solid line) and from the best fits of the KER distributions assuming a simple Arrhenius form (dotted and dashed lines).

is very satisfactory, confirming in this new but important case that phase space theory is accurate as long as statistical observables are concerned. The agreement also shows that the $-C_4/(r - r_0)^4$ dissociation potential is appropriate, confirming that the centrifugal barriers are low and located at long distances. The results shown here and below for Ar_{14}^+ remain essentially unchanged if the simpler $-C_4/r^4$ dissociation potential is used.

The variations of the average KER with excitation energy, represented in the inset of Figure 6, reveal a small backbending at 0.08 eV extra energy above the dissociation threshold, in agreement with the thermodynamical caloric curve computed from independent microcanonical Monte Carlo calculations (see below).

In Figure 6, we have superimposed the best fits of the KERD as $f(\epsilon) \propto \epsilon^\alpha \exp(-\epsilon/k_BT)$ with $\alpha = 1$ and $\alpha = {}^1/_2$. While the fit obtained for $\alpha = {}^1/_2$ cannot be distinguished from the PST curve, a significant deviation is observed when assuming the larger value for α. The nice fit obtained for $\alpha = {}^1/_2$ is obviously not surprising, since this value should be appropriate for an ion/neutral reaction. Finally, we notice that the typical average KER and the KER distribution found here agree well with the experimental data reported by Woodward and Stace.[56]

3. Calorimetric Measurements. The microcanonical temperature T_μ of the product cluster Ar_{13}^+ was obtained from the vibrational density of states using the same standard techniques. Its variations with excess energy are represented in Figure 7, along with temperatures extracted from the KER distributions. As in the case of neutral clusters, we calculate T_μ by assuming an Arrhenius form $\epsilon^\alpha \exp(-\epsilon/k_BT_\mu)$ for the KERD or from the moments only. The temperature shows a convex part near the excess energy of 0.08 eV, which is indicative of the solidlike−liquidlike phase change similar to that found in neutral clusters.

The poor fit obtained for the power $\alpha = 1$ is reflected in the large deviations between the fitted temperature and the thermodynamical value. The relative error for this estimate exceeds 40% in the entire energy range, which is again similar to the results on the neutral cluster. In contrast, the temperatures extracted from the moments of the distribution or from a fit with power of ${}^1/_2$ lead to a much better agreement. However, even with these more correct approaches, the deviations remain quite large, about 20% on average. It thus seems that, while PST is quite good in reproducing the "exact" MD results, the approximations used in establishing the exponential form from the KERD distributions are not fully valid in general. As in the case of neutral clusters, some corrections are needed to improve the assumed expression of the KERD, in order to extract temperatures that are closer to the actual thermodynamical value.

C. Possible Improvements. As was mentioned in section II, the large size approximation is crucial to establish the Arrhenius form of the KER distribution in two respects, namely, the Taylor expansion of the VDOS itself and the neglect of the (second-order) heat capacity term. As a matter of fact, the comparison between the temperatures extracted from the KERD and the thermodynamical value is much more favorable for the larger cluster Ar_{56} than for Ar_{14}. We wish to discuss here some alternative forms for the KER distributions that could improve the quality of the measurements, especially for small systems.

Starting from the most general PST/OTS expression of eq 2 in which we take $\partial\Gamma/\partial\epsilon_r =$ constant, another form for the KER distribution, better than eq 5 and valid up to second order in ϵ_{tr}, can be found by writing

$$\omega(E - E_0 - \epsilon_t - \epsilon_r) \simeq \omega(E - E_0)\left(1 - \frac{k_B}{C}\frac{\epsilon_{tr}^2}{2k_B^2T_\mu^2}\right)\exp(-\epsilon_{tr}/k_BT_\mu) \quad (10)$$

Inserting this expression into eq 2 leads to

$$f(\epsilon_t) = \omega(E - E_0)k_BT_\mu \exp\left(-\frac{\epsilon_t}{k_BT_\mu}\right)\left\{1 - e^{-A/k_BT_\mu} - \frac{k_B}{2C}\left[\left(\frac{\epsilon_t}{k_BT_\mu}\right)^2 - \frac{\epsilon_t^2 + A^2}{k_B^2T_\mu^2}e^{-A/k_BT_\mu} + 2\left(1 + \frac{\epsilon_t}{k_BT_\mu}\right)\left(1 - e^{-A/k_BT_\mu} - \frac{A}{k_BT_\mu}e^{-A/k_BT_\mu}\right)\right]\right\} \quad (11)$$

While this expression is general and free of most approximations, it is not quite tractable in practice.

(A2′) To make the above expression useful, we assume that $A \ll k_BT_\mu$ for all values of ϵ_t. We get

$$f(\epsilon_t) \approx A(\epsilon_t)\, e^{-\epsilon_t/k_BT_\mu}\left[1 - \frac{k_B}{2C}\left(\frac{\epsilon_t}{k_BT_\mu}\right)^2\right] \quad (12)$$

If we keep the explicit form $A(\epsilon_t) = \Lambda\epsilon_t^\alpha$, the last equation and eq 6 can be considered better possible forms for the KER distribution. The approximations they refer to, respectively, (A2) and (A2′), are different. (A2) involves a thermodynamical approximation that the heat capacity is much larger than k_B. On the other hand, (A2′) is related to the mechanical constraints associated with the conservation of the zero angular momentum, namely, that the rotational energy of the product is sufficiently small. As we have shown in section II, both approximations rely on the assumption that the number of degrees of freedom is large ($C \sim 3nk_B \gg k_B$ and $A \sim n^{-4/3}$ or $A \sim n^{-5/3}$, hence $A \ll k_BT_\mu$).

We have repeated the extraction of the product temperature from the KERD, but imposing now the forms of eq 6 or eq 12 instead of the basic Arrhenius expressions. The results for Ar_{14} and Ar_{14}^+ are represented in Figure 8. Any of the two new forms appears to be better than the Arrhenius behavior, but it looks obvious that the most critical approximation is (A2) concerning the range of available rotational energies. In general, the relative error in the estimated temperature decreases by a factor of at least 2 when giving up approximation (A2), while it decreases

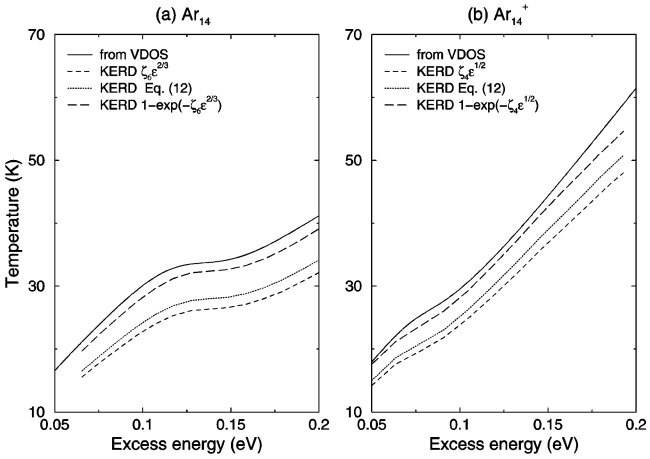

Figure 8. Temperature of the product clusters Ar_{13} (left panel) and Ar_{13}^+ (right panel) obtained from fitting the KER distribution by forms alternative to the simple Arrhenius expression vs excess energy. Solid line, reference Monte Carlo data; dotted lines, Arrhenius form; dashed lines, heat capacity corrections, eq 12; long dashed lines, the prefactor $\zeta_p\epsilon^\alpha$ where $\zeta_p = \Lambda_p/k_BT$ is replaced by the less approximate $1 - \exp(-\zeta_p\epsilon^\alpha)$.

by a few percentage points only when accounting for the finite heat capacity in (A2′).

The observation that both approximations contribute to an improvement in the estimated temperatures suggests an empirical form for the KERD that accounts simultaneously for the heat capacity correction as well as the possibly large maximum rotational energy. This new expression combines the two approximations (A2) and (A2′) in the following way:

$$f(\epsilon_t) \approx \left[1 - \exp\left(-\frac{\Lambda_p \epsilon_t^{(p-2)/p}}{k_B T_\mu}\right)\right]\left[1 - \frac{k_B}{2C}\left(\frac{\epsilon_t}{k_B T_\mu}\right)^2\right] \exp\left(-\frac{\epsilon_t}{k_B T_\mu}\right) \quad (13)$$

We have verified that this expression indeed improves the agreement between the thermodynamical temperature and the value fitted from the KERD. Since both the interaction constant Λ_p and the heat capacity C can be easily estimated, we expect the form of eq 13 to be particularly useful in the experimental determination of temperatures from the translational energy released.

IV. Conclusion

Kinetic energy released distributions from dissociating clusters potentially contain a lot of information about the thermodynamical state of the products. Following previous authors, particularly Klots[23−26] and Chesnavich and Bowers,[28] and building upon cluster specific studies,[38−42] we have extended our work on statistical theories of dissociation[43−46] by focusing on the KERD observable. The distribution of KER is particularly relevant in experiments, because it does not incorporate as many free parameters as, e.g., the reaction rates. Our present motivation was to question whether the thermodynamical properties (internal temperature) could be actually extracted from the KERD. This question was addressed from the point of view of phase space theory in its orbiting state formalism. By performing large scale molecular dynamics simulations on neutral and charged argon clusters, we were able to confirm the general validity of PST/OTS for the reproduction and prediction of KER distributions. The statistical theory was used in turn to provide benchmark data, to assess the reliability of the Arrhenius form $f(\epsilon) \propto \epsilon^\alpha \exp(-\epsilon/k_BT)$ assumed for the KERD. In this purpose, approximations leading from the rigorous PST treatment to the Arrhenius form were progressively introduced. Our numerical simulations allowed us to critically discuss the validity of these approximations.

In general, we found that size effects play an important role, with the Arrhenius expression being more relevant for large systems for which the hypothesis that the KER is much smaller than the excess energy holds. The maximum rotational energy also decreases with increasing sizes, even though its variations depend on the nature of the interaction between the products. For clusters containing several tens of atoms, the Arrhenius form was seen to be generally correct, provided that the appropriate power α was included in the fitting expression. In this respect, the temperature obtained from the second moment of the KER distribution is seen to be much better than the value given when assuming the (incorrect) hard core value $\alpha = 1$. However, for the 14-particle neutral and charged argon clusters, significant deviations ranging up to more than 40% between the thermodynamical temperature and the value fitted from the KERD were observed when using a simple Arrhenius form. These deviations are related to the breakdown of some specific approximations. At least two improvements have been proposed that should allow much better estimates of the cluster temperature from the KERD. We expect these improvements to be of straightforward use in most experiments, and we plan to apply the present suggestions to the case of thermionic electron emission.[35,36]

The present work was limited to spherical clusters at fixed total energy and zero angular momentum. Nonspherical clusters or the dissociation of molecules could be treated as well, even though the expressions for the rotational densities of states often become cumbersome.[28] Most of the present results could be also extended to a finite angular momentum. However, for rotating clusters, the centrifugal barrier could be significantly higher and located more closely to small distances. This would require a better knowledge of the dissociation potential, especially in the case of charged clusters where the $-C/r^4$ polarization interaction may not be fully appropriate, even when it is modified into $-C_4/(r - r_0)^4$ to account for the finite extent of the cluster.

The practical situation of thermalized clusters would need further work, as the thermal energy distributions of the parent cluster would have to be accounted for. The description of clusters prepared cold and excited through a collision or by photoabsorption also calls for a more complete modeling. In the case of a laser excitation, or if the collision is highly energetic, the influence of the excited states during at least the first stages of the dynamics could be a determining factor.

Acknowledgment. Financial support from the GDR Agrégats, Dynamique et Fragmentation is gratefully acknowledged.

References and Notes

(1) Ellert, C.; Schmidt, M.; Schmitt, C.; Reiners, T.; Haberland, H. *Phys. Rev. Lett.* **1995**, *75*, 1731.

(2) Honea, E.; Homer, M.; Persson, J. L.; Whetten, R. L. *Chem. Phys. Lett.* **1990**, *171*, 147.

(3) Branz, W.; Malinowski, N.; Schaber, H.; Martin, T. P. *Chem. Phys. Lett.* **2000**, *328*, 235.

(4) Gspann, J. In *Physics of Electronic and Atomic Collisions*; Datz S., Ed.; North-Holland: Amsterdam, 1986.

(5) Schmidt, M.; Kusche, R.; Kronmüller, W.; von Issendorff, B.; Haberland, H. *Phys. Rev. Lett.* **1997**, *79*, 99. Schmidt, M.; Hippler, T.; Donges, J.; Kronmüller, W.; von Issendorff, B.; Haberland, H.; Labastie, P. *Phys. Rev. Lett.* **2001**, *87*, 203402. Haberland, H.; Hippler, T.; Donges, J.; Kostko, O.; Schmidt, M.; von Issendorff, B. *Phys. Rev. Lett.* **2005**, *94*, 035701.

(6) Gobet, F.; Farizon, B.; Farizon, M.; Gaillard, M. J.; Buchet, J. P.; Carré, M.; Scheier, P.; Märk, T. D. *Phys. Rev. Lett.* **2002**, *89*, 183403.

(7) Bréchignac, C.; Cahuzac, Ph.; Concina, B.; Leygnier, J. *Phys. Rev. Lett.* **2002**, *89*, 203401.
(8) Brockhaus, P.; Wong, K.; Hansen, K.; Kasperovich, V.; Tikhonov, G.; Kresin, V. V. *Phys. Rev. A* **1999**, *59*, 495.
(9) Shvartsburg, A. A.; Jarrold, M. F. *Phys. Rev. Lett.* **2000**, *85*, 2530. Breaux, G. A.; Benirschke, R. C.; Sugai, T.; Kinnear, T. S.; Jarrold, M. F. *Phys. Rev. Lett.* **2003**, *91*, 215508. Breaux, G. A.; Neal, C. M.; Cao, B.; Jarrold, M. F. *Phys. Rev. Lett.* **2005**, *94*, 173401.
(10) Martinet, G.; Díaz-Tendero, S.; Chabot, M.; Wohrer, K.; Della Negra, S.; Mezdati, F.; Hamrita, H.; Désesquelles, P.; Le Padellec, A.; Gardés, D.; Lavergne, L.; Lalu, G.; Grave, X.; Clavelin, J. F.; Hervieux, P.-A.; Alcamí, M.; Martín, F. *Phys. Rev. Lett.* **2004**, *93*, 063401.
(11) Shulz, C. P.; Haugstätter, R.; Tittes, H. U.; Hertel, I. V. *Phys. Rev. Lett.* **1986**, *57*, 1703.
(12) Laskin, J.; Lifshitz, C. *J. Mass. Spectrom.* **2001**, *36*, 459.
(13) Engelking, P. C. *J. Chem. Phys.* **1987**, *87*, 936.
(14) Bréchignac, C.; Cahuzac, Ph.; Leygnier, J.; Weiner, J. *J. Chem. Phys.* **1989**, *90*, 1492.
(15) Atrill, S.; Stace, A. J. *J. Chem. Phys.* **1998**, *108*, 1924.
(16) Choi, H.; Bise, R. T.; Hoops, A. A.; Mordaunt, D. H.; Neumark, D. M. *J. Phys. Chem. A* **2000**, *104*, 2025.
(17) Borggreen, J.; Hansen, K.; Chandezon, F.; Døssing, T.; Elhajal, M.; Echt, O. *Phys. Rev. A* **2000**, *62*, 013202.
(18) Weitzel, K.-M.; Mähnert, J. *Int. J. Mass. Spectrom.* **2002**, *214*, 175 and references therein.
(19) Gluch, K.; Matt-Leubner, S.; Echt, O.; Concina, B.; Scheier, P.; Märk, T. D. *J. Chem. Phys.* **2004**, *121*, 2137.
(20) Jarrold, M. F. Introduction to statistical reaction theories. In *Clusters of Atoms and Molecules I*; Haberland, H., Ed.; Springer: Berlin, 1991.
(21) Weisskopf, V. *Phys. Rev.* **1937**, *52*, 295.
(22) Rice, O. K.; Ramsperger, H. C. *J. Am. Chem. Soc.* **1928**, *50*, 617. Kassel, L. S. *J. Phys. Chem.* **1928**, *32*, 225.
(23) Klots, C. E. *J. Phys. Chem.* **1971**, *75*, 1526.
(24) Klots, C. E. *J. Chem. Phys.* **1976**, *64*, 4269.
(25) Klots, C. E. *J. Chem. Phys.* **1985**, *83*, 5854.
(26) Klots, C. E. *J. Phys. Chem.* **1992**, *96*, 1733.
(27) Troe, J. *J. Chem. Phys.* **1983**, *79*, 6017.
(28) Chesnavich, W. J.; Bowers, M. T. *J. Chem. Phys.* **1977**, *66*, 2306.
(29) Nikitin, E. *Theor. Exp. Chem.* **1965**, *1*, 83; **1965**, *1*, 90.
(30) Pechukas, P.; Light, J. C. *J. Chem. Phys.* **1965**, *42*, 3281.
(31) Mintz, D. M.; Baer, T. *J. Chem. Phys.* **1976**, *65*, 2407.
(32) Carter, D. E. *J. Chem. Phys.* **1976**, *65*, 2584.
(33) Campbell, E. E. B.; Levine, R. D. *Annu. Rev. Phys. Chem.* **2000**, *51*, 65.
(34) Andersen, J. U.; Bonderup, E.; Hansen, K. *J. Phys. B* **2002**, *35*, R1.
(35) Baguenard, B.; Pinaré, J. C.; Bordas, C.; Broyer, M. *Phys. Rev. A* **2001**, *63*, 023204.
(36) Lépine, F.; Bordas, C. *Phys. Rev. A* **2004**, *69*, 053201.
(37) Matt, S.; Echt, O.; Scheier, P.; Märk, T. D. *Chem. Phys. Lett.* **2001**, *348*, 194.
(38) Weerasinghe, S.; Amar, F. G. *J. Chem. Phys.* **1993**, *98*, 4967.
(39) Peslherbe, G. H.; Hase, W. L. *J. Chem. Phys.* **1994**, *101*, 8535.
(40) Peslherbe, G. H.; Hase, W. L. *J. Chem. Phys.* **1996**, *104*, 9445.
(41) Peslherbe, G. H.; Hase, W. L. *J. Chem. Phys.* **1996**, *105*, 7432.
(42) Peslherbe, G. H.; Hase, W. L. *J. Phys. Chem. A* **2000**, *104*, 10556.
(43) Calvo, F.; Parneix, P. *J. Chem. Phys.* **2003**, *119*, 256. Parneix, P.; Calvo, F. *J. Chem. Phys.* **2003**, *119*, 9469.
(44) Calvo, F.; Parneix, P. *J. Chem. Phys.* **2004**, *120*, 2780.
(45) Parneix, P.; Bréchignac, Ph.; Calvo, F. *Chem. Phys. Lett.* **2003**, *381*, 471.
(46) Parneix, P.; Calvo, F. *J. Chem. Phys.* **2004**, *121*, 11088.
(47) Stace, A. J. *J. Chem. Phys.* **1991**, *93*, 6502.
(48) Wüest, A.; Merkt, F. *J. Chem. Phys.* **2004**, *120*, 638.
(49) Ferrenberg, A. M.; Swendsen, R. H. *Phys. Rev. Lett.* **1988**, *61*, 2635.
(50) Pearson, E. M.; Halicioglu, T.; Tiller, W. A. *Phys. Rev. A* **1985**, *32*, 3030.
(51) Berry, R. S.; Jellinek, J.; Natanson, G. *Chem. Phys. Lett.* **1984**, *107*, 227.
(52) Brink, D. M.; Stringari, S. *Z. Phys. D: At. Mol. Clusters* **1990**, *15*, 257.
(53) Frauendorf, S. *Z. Phys. D: At. Mol. Clusters* **1995**, *35*, 191.
(54) Langevin, P. *Ann. Chim. Phys.* **1905**, *5*, 245.
(55) Stace, A. J.; Lethbridge, P. G.; Upham, J. E.; Woodward, C. A. *J. Chem. Soc., Faraday Trans.* **1990**, *86*, 2405.
(56) Woodward, C. A.; Stace, A. J. *J. Chem. Phys.* **1991**, *94*, 4234.
(57) Galindez, J.; Calvo, F.; Paska, P.; Hrivnak, D.; Kalus, R.; Gadéa, F. X. *Comput. Phys. Commun.* **2002**, *145*, 126 and references therein.
(58) Kuntz, P. J. Valdorf, J. *Z. Phys. D: At. Mol. Clusters* **1988**, *8*, 195.